Int J Earth Sci (Geol Rundsch) (2017) 106:1409–1427
DOI 10.1007/s00531-017-1469-6

ORIGINAL PAPER

# Provenance and paleogeography of the Mesozoic strata in the Muang Xai Basin, northern Laos: petrology, whole-rock geochemistry, and U–Pb geochronology constraints

**Yanlu Wang[1,2] · Licheng Wang[2] · Yushuai Wei[1] · Lijian Shen[2] · Ke Chen[1] · Xiaocan Yu[2] · Chenglin Liu[2]**

Received: 28 December 2016 / Accepted: 9 March 2017 / Published online: 30 March 2017


**Abstract** The Muang Xai Basin, located in northern Laos, is associated with the Simao, Vientiane, and Khorat Basins. The paleogeographic link of these basins has not been investigated in great detail; thus, the investigation presented in this study is a comprehensive analysis of petrology, whole-rock geochemistry, and detrital zircon U–Pb chronology used to characterize the provenance of the Muang Xai Basin. Results suggest that the sedimentary source includes felsic rocks from an active continental margin or continental arc with minor amounts of recycled passive continental margin sediments. Sandstones of the Muang Xai Basin contain detrital zircons with varying U–Pb peak ages. The youngest age peak of all the zircons is 103 Ma, which limits the age of the Mesozoic strata to the Late Cretaceous. Detrital zircon U–Pb and trace element data, combined with geochemical result, reveal that the pre-Ordovician zircons were derived from recycled sediments of the Yangtze Block, which are originally sourced from the Qinling Orogenic belt. This provenance is shared with coeval sediments in the Simao and Khorat Basins, while magmatic rocks of the Ailaoshan, Truong Son Belt, and Lincang terrane are responsible for zircons of 416–466 and 219–308 Ma in age. Zircons of 101–110 and 149–175 Ma in age were sourced from magmatic rocks of the southwestern South China Block and northern Vietnam. These provenance results suggest that sediments flow into the Khorat red beds was likely from the Great Simao Basin and northern Vietnam, and not directly from the Yangtze Block.

**Keywords** Provenance · Paleogeography · U–Pb detrital zircon age · Late Cretaceous · Muang Xai

## Introduction

Laos is located in the north of mainland SE Asia and the Muang Xai Basin, located in northern Laos, crops out as a succession of Mesozoic continental red beds (Department of Geology and Mines of Lao P.D.R. (DGM) 1991). These red beds are comparable to those in the Simao Basin (Wang et al. 2014), and the Muang Xai Basin forms an important zone that connects the Simao, Vientiane, and Khorat Basins in Laos and Thailand that contain one of the largest global potash resources (Hite and Japakasetr 1979). The genetic relationship between these basins and their paleogeographic link has been of great interest (Xu and Wu 1983; BGMRY 1986; Racey et al. 1996; Qu 1997; Qu et al. 1998; Racey 2009; Han et al. 2011; Morley 2012; Wang et al. 2014; Sinsoupho et al. 2014, 2015). However, there is little robust evidence of the paleogeographic link between them. Carter and Bristow (2003) indicated that the Khorat Basin was adjacent to the Sichuan Basin during the Early Cretaceous and that the source of the Khorat Group sediments was the Qinling Orogenic Belt. This argument is also suggested by Singsoupho et al. (2014, 2015). However, Wang et al. (2014) suggested that the Simao Basin was situated on the western margin of the Khorat Basin during the Late Cretaceous, and the source of the Khorat sediments was

**Electronic supplementary material** The online version of this article (doi:10.1007/s00531-017-1469-6) contains supplementary material, which is available to authorized users.

✉ Licheng Wang
wayne-wlc3@126.com

[1] School of Earth Science and Resources, China University of Geosciences, Beijing 100083, China

[2] MLR Key Laboratory of Metallogeny and Mineral Assessment, Institute of Mineral Resources, Chinese Academy of Geological Sciences, Beijing 100037, China

likely from Simao Basin. Therefore, the provenance and paleogeography of the equivalent strata in the Muang Xai Basin are significant for understanding the link between the Khorat and Simao basins.

Zircon is a highly refractory mineral that can endure cycles of geologic history with little to no alteration. For the past two decades, detrital zircon analysis has been used with increasing success to evaluate provenance and paleogeography and developing tectonic reconstructions (e.g., Fedo et al. 2003; Gehrels 2012). Interpretation of provenance based on detrital zircons can also be used to develop a geological history of sedimentary basins and their surrounding source regions (Fedo et al. 2003). A combination of U–Pb ages and trace elements of such detrital zircons can effectively constrain the sources and origins of detrital zircon grains in sedimentary rocks on a temporal basis (e.g., Wu et al. 2007, 2010; Hoang et al. 2009; Wang et al. 2015).

Furthermore, petrological analysis can be used to obtain the compositional characteristics and provenance of rock debris in a sedimentary basin (Dickinson et al. 1983), while whole-rock geochemistry can be applied to provenance analysis and discrimination of tectonic setting (Bhatia 1983; Bhatia and Crook 1986). In this study, an integrated approach based on petrology, whole-rock geochemistry, detrital zircon U–Pb age, and zircon trace element analysis is used to constrain the sedimentary provenance of Late Cretaceous strata of the Muang Xai Basin. This has further implications in terms of the paleogeography of the Simao and the Khorat Basins.

## Geological setting

Mainland SE Asia contains a complex assemblage of several Gondwana-derived micro-continents. This includes the South China Block (SCB), Indochina Block, Sibumasu Block, Sukhothai Block, and the Qamdo-Simao Block. These all experienced heterogeneous collisions during multiple closures of the Tethyan Ocean from the Late Permian to the Early Triassic (see reviews in Metcalfe 2011, 2013 and Fig. 1). The boundaries between these blocks consist of major fault zones and sutures such as the Red River Fault, Dien Bien Phu Fault, Jinghong Suture, Nan Suture, Song Ma Suture, and Ailaoshan Suture (Fig. 1). The evolution of the Tethyan Ocean is closely linked with collision of all these blocks mentioned above, also known as the Indosinian Orogeny (Wang et al. 2014 and references therein). During the Triassic, the collision of the SCB and North China Block led to the generation of the Qinling Orogenic Belt. To the north of the Ailaoshan suture, the closure of the Tethyan Ocean contributed to the collision between the Yidun terrane and Songpan-Ganzi terrane (SGT) in the Triassic (Wang et al. 2000, 2013). The Baoshan–Sibumasu Block collided with the Indochina Block after subduction of the Devonian–Triassic Tethys Ocean, and major suture zones are recognized, including the Jinghong and Nan sutures and the Changning-Menglian and the Inthanon sutures (Sone and Metcalfe 2008) (Fig. 1).

The Indochina Block is one of the largest tectonic units in SE Asia and occupies most of the Indochina peninsula. It is believed to have been extruded along the Red River fault by the collision between India and Asia during the Cenozoic (Tapponnier et al. 1982). The Indochina block borders the SCB along the Ailaoshan and Song Ma sutures to the north and northeast, and is separated from the Baoshan–Sibumasu Block by the Lincang granites, Sukhothai Arc, and the Inthanon Suture Zone in the west (Sone and Metcalfe 2008; Metcalfe 2011). Like other continental blocks in SE Asia, the Indochina Block is thought to have been proximal to Gondwana during the Early Paleozoic (Metcalfe 2011, 2013). Paleomagnetic studies have been used to identify different internal rotational deformations in the Indochina Block (Chen et al. 1995; Sato et al. 1999, 2007; Tong et al. 2013), which has also been thoroughly transected by some Neogene strike-slip faults such as the Dien Bien Phu Fault and the Ailaoshan-Red River Fault (Wang et al. 2016).

The Simao Basin, located in the southern part of Qamdo-Simao block, is a continental rift basin during the Jurassic–Cretaceous period (Qu et al. 1998). The Qamdo–Simao block is bounded by the Jinghong and Nan suture zones in the west and the Jinshajiang, Ailaoshan, and Song Ma sutures in the east (Sone and Metcalfe 2008; Metcalfe 2011). The collision of the Simao and SCB occurred in the Late Triassic (Jian et al. 2009) or Late Permian–Early Triassic (Metcalfe 2009).

The Nan-Dien Bien Phu Suture Zone and the Truong Son Belt are two tectonic boundaries of the magmatic and sedimentary rocks in northern Laos (Wang et al. 2016). Mesozoic strata, cropped out in the Muang Xai Basin, have not been sufficiently subdivided due to the limited geological mapping data (Fig. 2a; DGM 1991). The Mesozoic outcrops (MZ1, MZ2, DGM 1991) are mainly purple and red continental mudstones interbedded with red siltstones and sandstones, with clay conglomerates and gypsum (Figs. 2, 3). The lithological association is comparable to the Late Cretaceous Mengyejing Formation in the Simao Basin and believed to have been deposited in a lacustrine basin (Wang et al. 2014, 2015). The Mengyejing Formation can be divided into three members (Wang et al. 2015). The lower member consists of an evaporite-bearing (halite and gypsum) succession of red–brown clay conglomerates, mudstones, and sandstones. The middle member is mostly red–brown siltstones, mudstones interbedded with fine sandstones and yellow mudstones and marls. The lower part of the upper member is dominated by clay conglomerates,

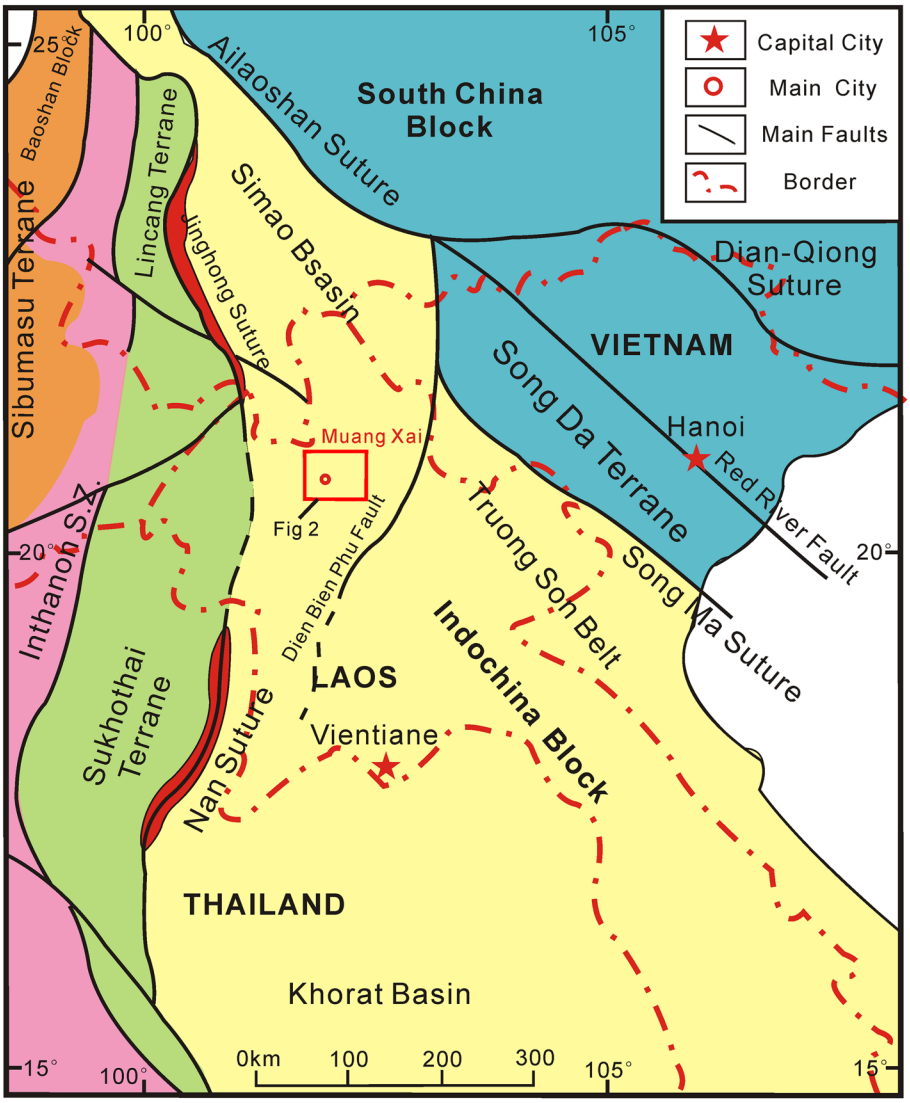


**Fig. 1** Tectonic framework of central SE Asia showing the location of the Muang Xai Basin (modified from Sone and Metcalfe 2008)

halite, sylvite, and gypsum interbedded with several tuff layers, and the upper part is mainly red–brown siltstones, mudstones, and sandstones. The Late Cretaceous continental red beds with evaporites are also present in the Khorat Basin (Racey 2009; Racey and Goodall 2009).

## Samples and analytical methods

The studied section of the Mesozoic strata is located at Muang Xai area, northern Laos (20°38.18′ −57.27′N; 102°1.3′ −33′E) (Figs. 2, 3) and believed as the equivalent of the Late Cretaceous Mengyejing Formation in the Simao Basin. Nine lithic sandstone samples were taken from the bottom of the section and selected for modal analysis and subjected to point-counts (>400 points per sample) following the Gazzi-Dickinson method (Ingersoll et al. 1984). The full dataset is presented in the supplementary material.

The major and trace element compositions of nine sandstone samples were analyzed at the Beijing Research Institute of Uranium Geology. Major element analysis was conducted using a Philips PW2404 X-ray fluorescence spectrometer (XRF) according to the method of Long et al. (2008) with an analytical accuracy of <1%. Trace element analysis was performed using an ELEMENT XR high-resolution inductively coupled plasma mass spectrometer (ICP-MS) using the analytical procedure is given by Cullen et al. (2001) with an analytical precision of <2.5%.

Six sandstone samples from the Mesozoic strata were collected for U–Pb geochronology and trace element analysis (Fig. 2a). All samples were selected from fresh, medium- to coarse-grained sandstones. A total of 150 representative zircon grains were selected using conventional heavy liquid and magnetic techniques. All grains were handpicked under a binocular microscope and mounted in a 25 mm epoxy-resin mount. The epoxy-resin was polished

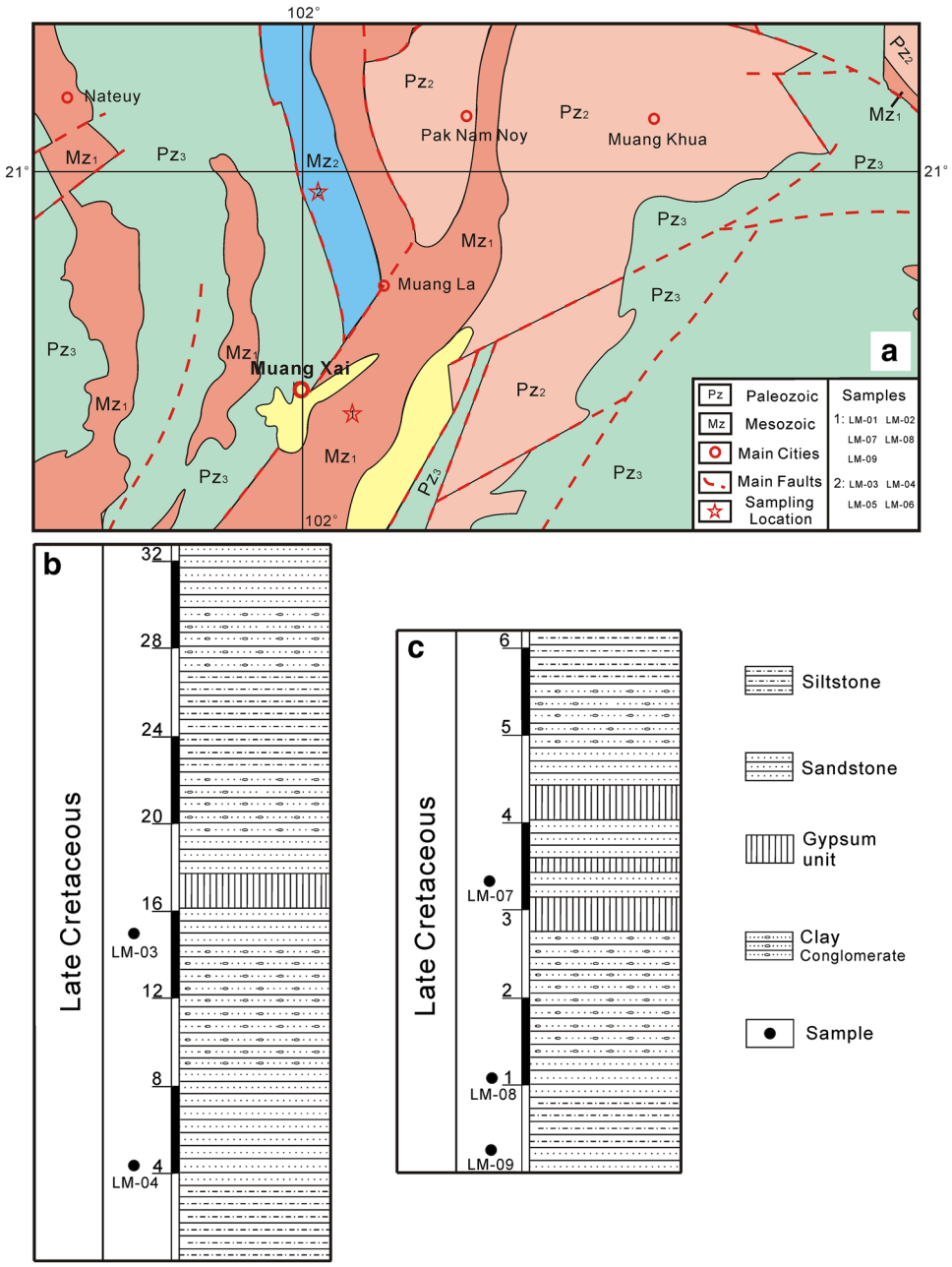


**Fig. 2** **a** Geological map of the Muang Xai Basin, Laos (Modified from Department of Geology and Mine, Laos P.D.R. (DGM) 1991); **b, c** Lithostratigraphic column of the Late Cretaceous section in the Muang Xai Basin

until most of the zircon grains were exposed and were then coated with gold film. Cathodoluminescence (CL) images of the zircons were taken at the Beijing SHRIMP (sensitive high-resolution ion microprobe) Center, Chinese Academy of Geological Sciences to reveal the internal growth structures of the zircon grains.

U–Pb dating and trace element analyses of the zircon were conducted synchronously by LA-ICP-MS at the State Key Laboratory of Geological Processes and Mineral Resources, China University of Geosciences, Wuhan. Detailed operating conditions and data reduction was completed according to the standard operating techniques described by Liu et al. (2008, 2010a, b). Laser sampling was performed using a GeoLas 2005. An Agilent 7500a ICP-MS instrument was used to acquire ion-signal intensities. U–Pb ages were calculated using the ICPMSDataCal (Liu et al. 2008, 2010a) with Zircon 91500 as an external standard (Wiedenbeck et al. 1995). Concordia diagrams and weighted mean calculations were calculated using Isoplot/Ex_ver3 (Ludwig 2003). The interpreted ages are based on the $^{206}Pb/^{238}U$ ratios for grains <1000 Ma grains and on the $^{207}Pb/^{206}Pb$ ratios for grains >1000 Ma (Pullen et al. 2008).


**Fig. 3** **a** Outcropped section in the Muang Xai Basin; **b** purple siltstones and mudstones, the length of the hammer is about 33 cm; **c** gypsum layers, siltstones, and clay conglomerates; **d** clay conglomerates

## Results

### Petrology

The studied sandstone strata of Muang Xai area consist mainly of quartz and lithic fragments (Fig. 4). Quartz is mostly monocrystalline grains with less amount of polycrystalline quartz, and sub-angular to angular in form. Some dissolution of quartz grains was also observed (Fig. 4c, d). Most samples have a high percentage of lithic fragments with a few feldspars (plagioclase > K-feldspar). Lithic fragments are mostly volcanic in origin, while two samples (LM-03 and LM-04) have a larger percentage of sedimentary fragments (Fig. 4e, f). Limestone and pelitic fragments are also observed and calcite cement is present in some samples (Fig. 4e). Heavy minerals such as zircon and opaque minerals (pyrite and hematite) were identified.

The nature of the parent rocks in the region from which sandy detritus was derived can be determined from the relative proportions of different sand grain types. Dickinson and Suczek (1979) proposed that the mean compositions of sandstone grains derived from different kinds of provenance regions controlled by plate tectonic processes are inclined to plot within discrete fields on QFL (quartz, feldspar, lithic fragments) and QmFLt (monocrystalline quartz, feldspar, total lithic fragments) diagrams.

Analyses of the Muang Xai samples are provided in Table A1 in the supplementary material. From the plot of recalculated values, it is evident that most of the samples plot in the recycled orogenic provenance field in the QFL plot with two samples in the undissected arc field (Fig. 5a). The QmFLt plot shows that the samples are consistent with a quartzose recycled provenance, with little contribution from the lithic recycled provenance (Fig. 5b). On a plot of LmLvLs (total metamorphic lithic fragments, total volcanic lithic, total sedimentary lithic fragments), the samples show compatibility with a magmatic arc and rifted continental margin provenance (Fig. 5c).

### Whole-rock geochemistry

The major and trace element compositions of samples from the Muang Xai Basin are listed in Table A2 in the supplementary material. The samples exhibit a large variation in chemical composition and $SiO_2$ content, which is in the 73.76–92.99 wt.% range (average of 86.09 wt%). This composition indicates enrichment relative to the upper continental crust (UCC, 65.89 wt%) (Taylor and McLennan 1985) with the exception of samples LM-03 (58.34 wt%)

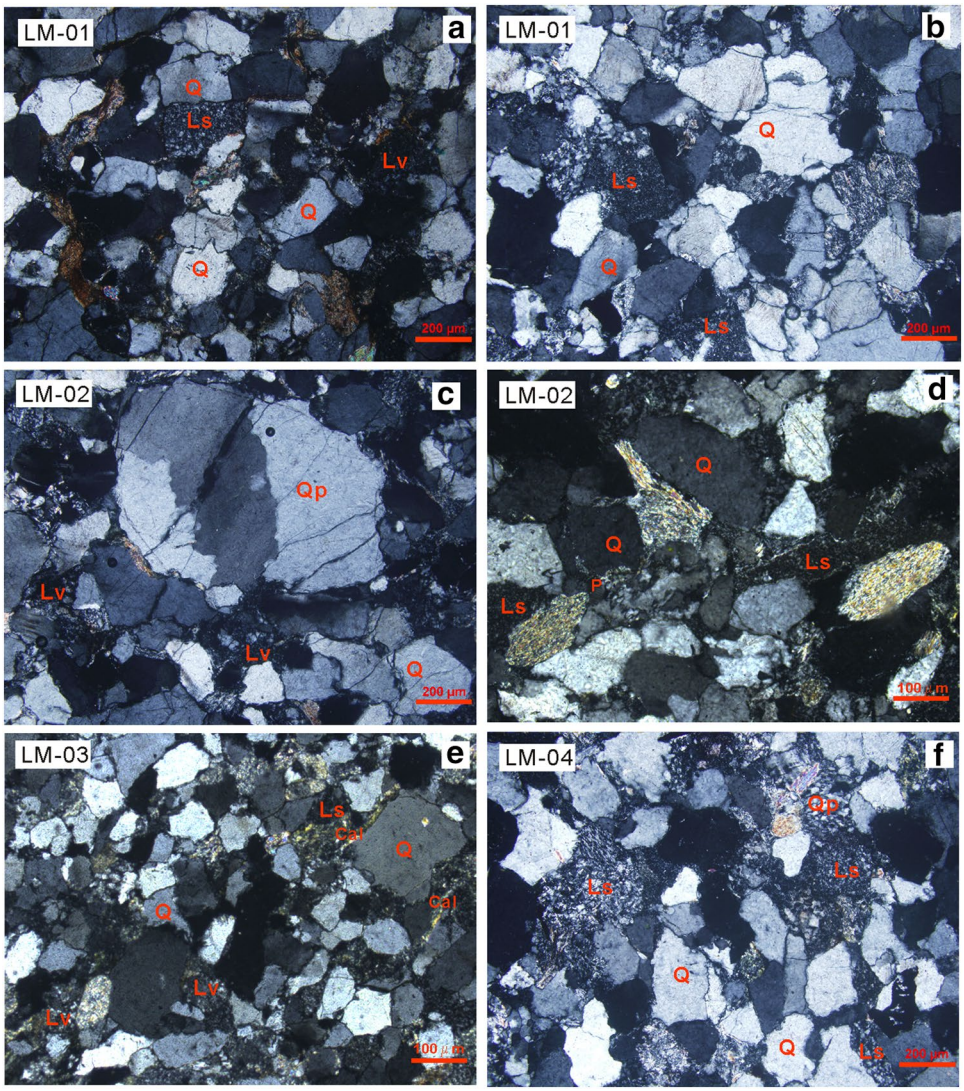


**Fig. 4** Photomicrographs of typical detritus of the Muang Xai sandstones under cross-polarized light. **a–d** Quartz and volcanic and sedimentary lithic fragments, samples LM-01, LM-02; **e** calcite cements, sample LM-03; **f** sedimentary rock fragments and polycrystalline quartz, sample LM-04. *Q* quartz, *Qp* polycrystalline quartz, *lv* volcanic lithic fragment, *Ls* sedimentary lithic fragment, *Cal* calcite

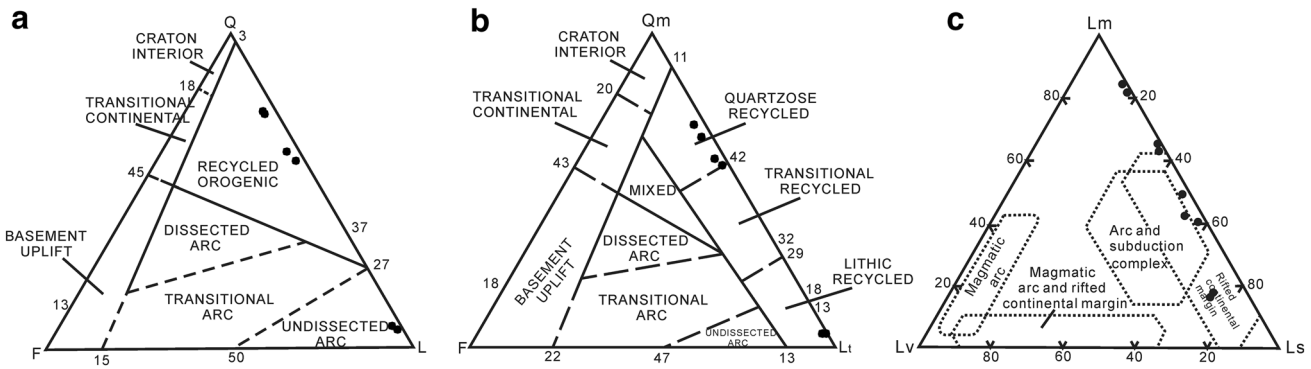


**Fig. 5** QFL (**a**), QmFLt (**b**), and LmLvLs (**c**) plots for framework modes of terrigenous sandstones showing provisional subdivisions according to inferred provenance type, modified after Dickinson and Suczek (1979). *Q* total quartz grains, *Qm* quartz grains that are exclusively monocrystalline, *F* total feldspar grains, *L* total unstable lithic fragments, *Lt* total polycrystalline lithic fragments, *Lm* metamorphic, *Lv* volcanic, *Ls* sedimentary lithic fragments, *Cal* calcite

and LM-04 (59.18 wt%). The $Al_2O_3$ concentrations (5.23–13.22 wt%, average of 8.26 wt%) are lower than that of the UCC (15.17 wt.%) and the post-Archean Australian shales (PAAS) (18.9 wt%, Taylor and McLennan 1985). Low CaO concentrations were observed in most samples, but several samples have concentrations up to 11.50 wt%, which is likely the result of their higher limestone fragment and calcite cement content (Fig. 4). All the samples contain much lower $Na_2O$ concentrations (average of 0.09 wt%) than the UCC.

Trace element compositions show that most samples are slightly enriched in refractory elements such as Hf, Zr, Cr, and U, and significantly depleted in Rb, Sr, Ba and Nb. Generally, the REE content ranges from 95.57 to 162.45 ppm with a median of 128.81 ppm that is lower than that of PAAS (211.76 ppm, Taylor and McLennan 1985). These samples are enriched in light rare earth element (LREE) and exhibit relatively flat heavy rare earth element (HREE) profiles. The LREE/HREE ratio is in the 6.73–12.36 range, while the $La_N/Yb_N$ ratio is in the 7.91–15.19 range, which indicates a large degree of fractionation between LREE and HREE. All the samples exhibit moderate negative Eu anomaly (Eu/Eu* of 0.58–0.71, average of 0.64) and slightly negative Ce anomalies (Ce/Ce* of 0.85–0.92, average of 0.89). The negative Eu anomaly is nearly identical to the value of 0.65 of the North American Shale Composite-NASC (Haskin and Haskin 1966).

## Zircon U–Pb isotopic ages

Six sandstone samples from the Late Cretaceous strata were analyzed for U–Pb ages of their detrital zircons. The zircon grains are typically rounded to subhedral in form, and are 50–120 μm in size. Oscillatory growth zones and inherited cores can be observed in the CL images (Fig. 6). Most zircons with oscillatory zoning can be regarded as being magmatic in origin. Most zircons have high Th/U ratios, which range from 0.09 to 2.04.

The U–Pb data are given in Table A3 in the supplementary material. The data show that 383 grains obtained from the six samples give concordant ages at the 90% confidence level, and analysis with discordance higher than 10% was not taken into consideration. The U–Pb data for all samples are presented in concordia diagrams (Fig. 7) and relative probability plots (Fig. 8). In all 383 grains, the youngest age is 101 Ma, and the oldest age is 3.37 Ga. The youngest cluster of ages is in the range of 101–110 Ma. There is another young peak of Jurassic ages (155 Ma), with ages in the 149–175 Ma range ($n = 13$). The 383 grains display two significant peaks at 248 Ma and 437 Ma, with 24% of the ages in the 219–308 Ma range ($n = 92$) and 16% in the 416–466 Ma range ($n = 62$). There is a subordinate peak at 1.83–1.85 Ga ($n = 13$, peak at 1.84 Ga) and others of two smaller groups of zircons in the 730–858 Ma range ($n = 25$) and 2.47–2.50 Ga ($n = 7$). The small rounded zircons are most likely polycyclic, derived from a source of several sedimentary cycles, and the euhedral grains are first-cycle zircons derived from crystalline basement (Carter and Bristow 2003). The Phanerozoic grains are most likely first-cycle zircons with euhedral morphology, and the Proterozoic and Archean grains are most likely polycyclic (Fig. 7).

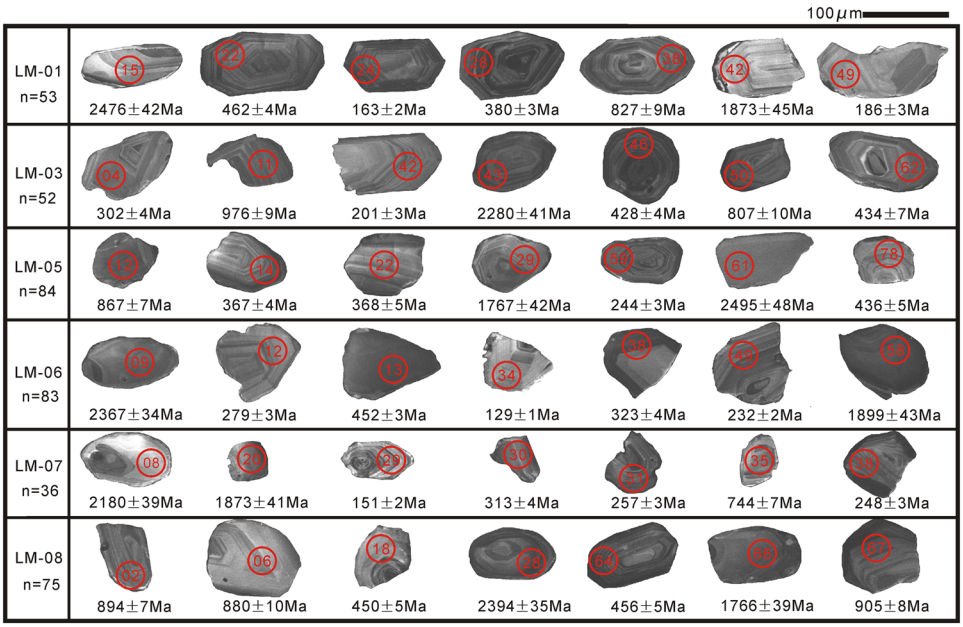


**Fig. 6** Representative Cathodoluminescence (CL) images for detrital zircons from the sandstone samples at Muang Xai. The laser spots and corresponding ages are marked

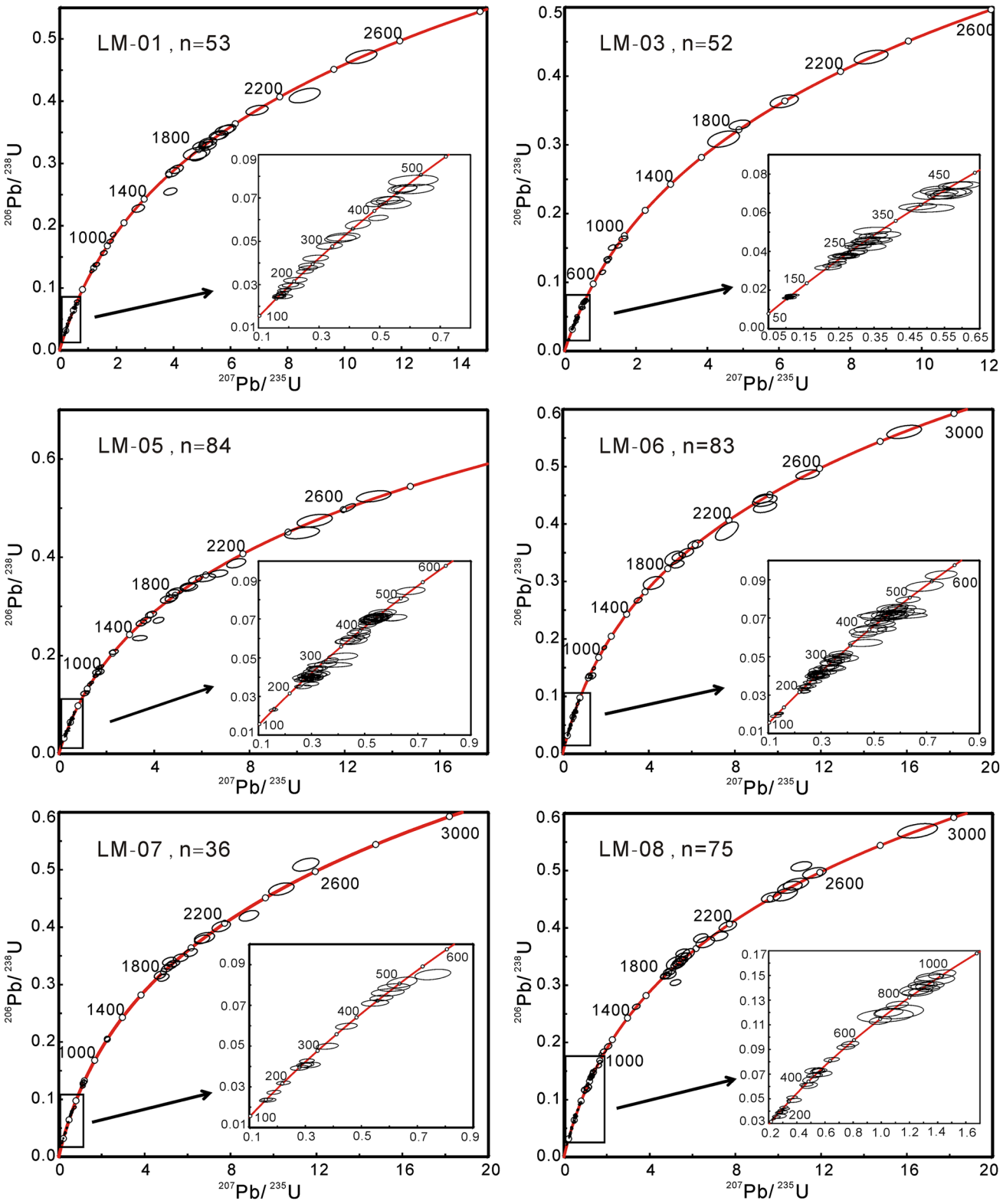


**Fig. 7** U–Pb concordia diagrams plots for samples of the Mesozoic sandstone from the Muang Xai Basin

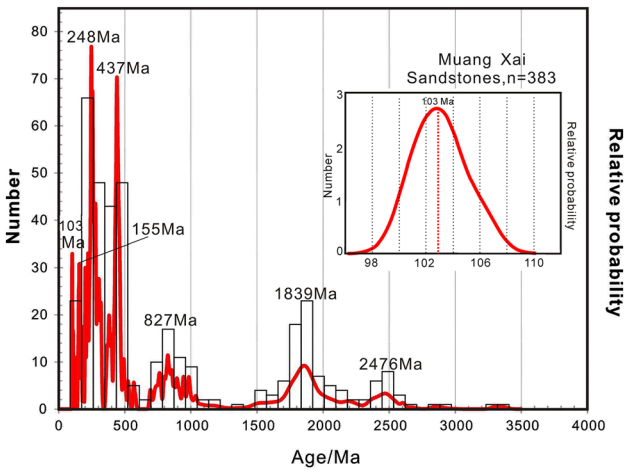


**Fig. 8** Age probability plots for samples of the Mesozoic sandstone from the Muang Xai Basin

## Detrital zircon trace elements

Trace element data of the detrital zircons is provided in Table A4. The trace element data provide significant information about the host rocks, such as compositional evolution, coexistence of fractionating phases, magma mixing processes, and characteristics of the zircon source region. Chondrite-normalized REE patterns for Precambrian to Early Paleozoic (Fig. 9a) and Late Paleozoic to Mesozoic detrital zircons (Fig. 9b) all have steep LREE ($Sm_N/La_N = 436.15$, averaging = 148.75) and flat HREE ($Lu_N/Gd_N = 25.48$, averaging = 18.41) patterns with positive Ce (Ce/Ce* = 28.18, averaging = 38.41) and small negative Eu anomalies (Eu/Eu* = 0.21, averaging = 0.25) (Fig. 9a, b). These patterns suggest a typical magmatic origin (Belousova et al. 2002; Hoskin and Schaltegger 2003), which is consistent with the Th/U ratio of 0.70.

The different geochemical composition of some trace elements (like Th, Hf and Nb) within zircon can be taken as reliable evidences to establish the tectonic settings of the host magma (Yang et al. 2012a). Within-plate settings

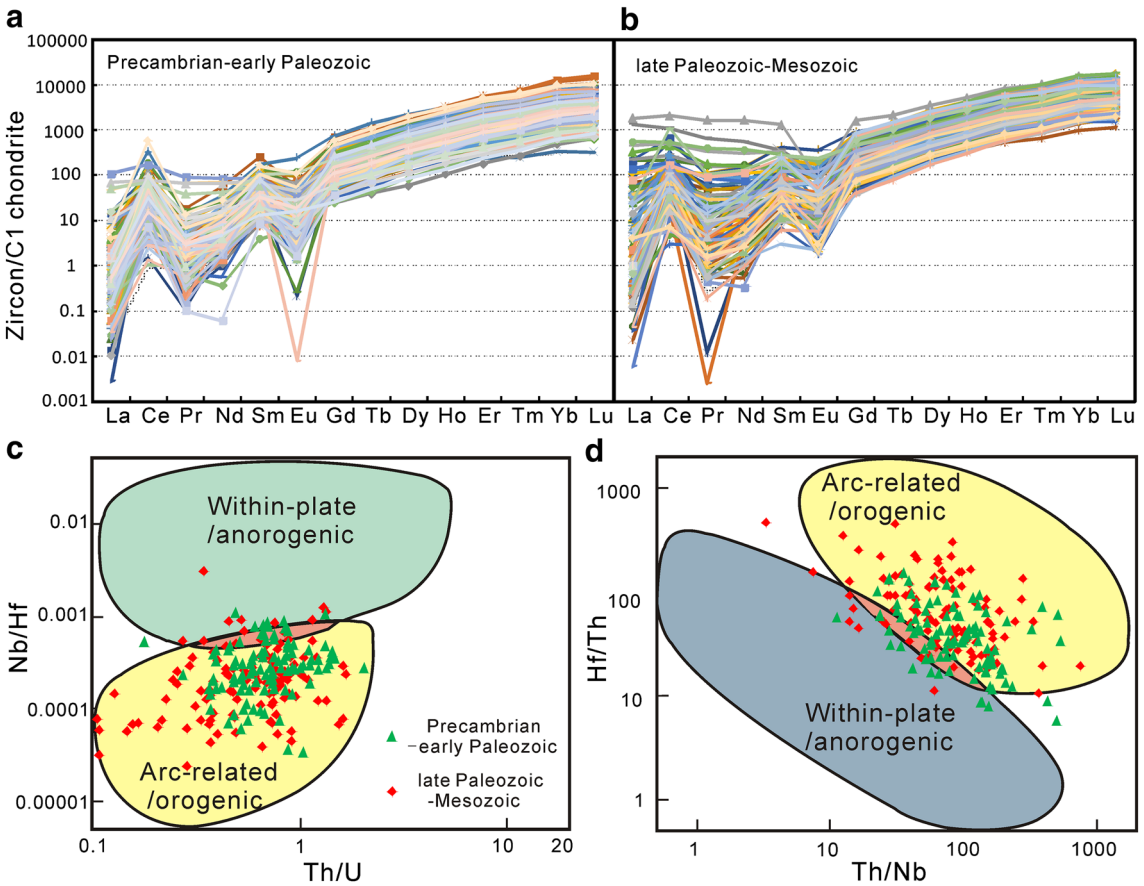


**Fig. 9** Chondrite-normalized REE patterns for detrital zircons of Precambrian-early Paleozoic ages (**a**); late Paleozoic–Mesozoic ages (**b**); magmatic zircon trace element discriminating diagrams of Th/U–Nb/Hf (**c**) and Th/Nb–Hf/Th (**d**). Chondrite REE values used for normalization in **a** and **b** are from Taylor and McLennan (1985) and within-plate/anorogenic and arc-related/orogenic fields in **c** and **d** were according to Yang et al. (2012a, b)

typically have less Nb than magmatic arc magmas, at a comparable degree of magmatic fractionation, and thus higher Th/Nb ratios and lower Nb/Hf ratios are expected for zircons originating from magmatic arcs compared with those from within-plate settings (Yang et al. 2012a). To characterize the source magma from which the magmatic zircons crystallized, the zircon trace element data were plotted on Th/U vs. Nb/Hf and Th/Nb vs. Hf/Th diagrams (Fig. 9c, d; Yang et al. 2012b). Most of the zircons with low Hf/Th ratios and Nb/Hf ratios plot in the arc-related/orogenic field, while some grains display high Hf/Th and Nb/Hf ratios that plot in the within-plate/anorogenic field (Fig. 9c, d). These results indicate that the magmatic rocks formed in a convergent tectonic environment determine the nature of potential sources (Yang et al. 2012b).

## Discussion

### Source-area weathering and sediment recycling

The geochemical characteristic of clastic sediment is the final result of many geological processes, such as source rock composition, intensity of physical and chemical weathering, the rate of sediment supply, and mineralogical/textural sorting during transportation and deposition (McLennan 1989; Cox et al. 1995). Weathering conditions are best evaluated before considering grain geochemistry (Roddaz et al. 2006) because both the major element geochemistry and mineralogy of siliciclastic sediments are affected by chemical weathering in the source area (Nesbitt and Young 1982, 1984; Fedo et al. 1995; Jorge et al. 2013). In this study, both the chemical index of alteration (CIA) (Nesbitt and Young 1982) and Index Chemical Variation (ICV) (Cox et al. 1995) are used to quantify the degree of weathering. The CIA was calculated using the molecular proportions as follows:

$$\mathrm{CIA} = [\mathrm{Al_2O_3}/(\mathrm{Al_2O_3} + \mathrm{CaO}* + \mathrm{Na_2O} + \mathrm{K_2O})] \times 100, \quad (1)$$

where CaO* is the amount of CaO incorporated in the silicate fraction of the rock. This is determined by a correction for calcium residing in carbonates and phosphates in which an actual value of $CO_2$ needs to be assumed (Bock et al. 1998). The formula $\mathrm{CaO}^* = \mathrm{CaO} - (10/3\mathrm{P_2O_5})$ was used to correct for the $P_2O_5$ content (apatite). If the mole fraction is such that $\mathrm{CaO} \leq \mathrm{Na_2O}$ after correcting for $P_2O_5$, then the value of CaO is accepted, but if the mole fraction is such that $\mathrm{CaO} \geq \mathrm{Na_2O}$, then the mole fractions of $Na_2O$ as CaO* is assumed. During weathering, the removal of labile cations (e.g., $Ca^{2+}$, $Na^{+}$, $K^{+}$) relative to stable residual constituents ($Al^{3+}$, $Ti^{4+}$) results in relatively high CIA values (>65–85) (Nesbitt and Young 1982). Conversely, low CIA values (<50–65) indicate the near absence of chemical alteration and consequently may reflect cool and/or arid conditions (Fedo et al. 1995). Unweathered igneous rocks typically have CIA values of 50 or less, while shales typically have average values of approximately 70–75 and residual clays have values near 100 (McLennan et al. 1993). The CIA values for the Muang Xai sandstones vary in the 75–87 range (average of 80), significantly higher than the average of approximately 50 for unweathered UCC (Taylor and McLennan 1985). This indicates moderate to intensive chemical weathering in the source area (Table A2).

The CIA diagram (Fig. 10) shows the degree of chemical weathering and its history in the source region (Nesbitt and Young 1982; Nyakairu and Koeberl 2001). The progressive alteration of plagioclase and potassium feldspars to form clay minerals can also be recorded by this diagram. Generally, intensive chemical weathering results in the formation of residual clays such as kaolinite and gibbsite that have high CIA values (76–100). Most data from the Muang Xai samples plot in the fields of intermediate and strong weathering, reflecting the presence of mature sands that contain quite degraded detrital feldspars from a relatively weathered or tectonically inactive source (Shao et al. 2012). The data spread suggests that the sediments may have derived from different chemical weathering sources.

As mentioned, the ICV method (Cox et al. 1995) can be used to measure the maturity and original composition of sandstones, as well as to study the tectonic setting. To measure the abundance of $Al_2O_3$ relative to the

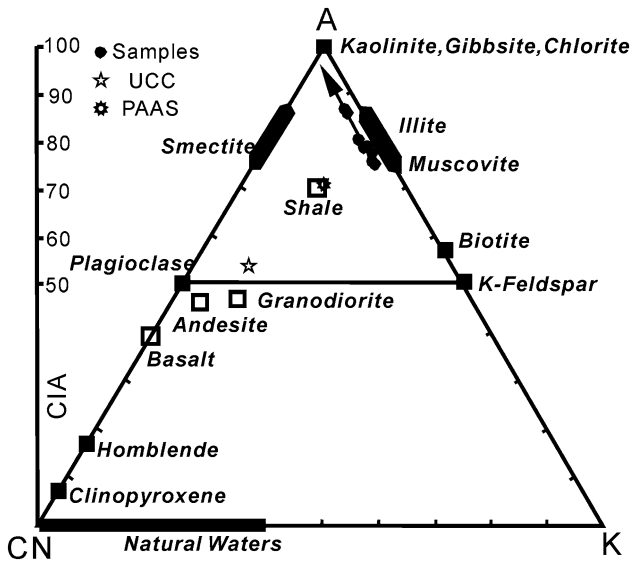


**Fig. 10** A–CN–K ($Al_2O_3$–CaO*+$Na_2O$–$K_2O$) ternary diagram (after Nesbitt and Young 1982, 1984, 1989) of the Muang Xai Basin samples. *UCC* average Upper Continental Crust from Taylor and McLennan (1985), *PAAS* post-Archean Australian Shale from Taylor and McLennan (1985)

other major cations in a rock or mineral, the ICV is usually defined as $[(Fe_2O_3 + K_2O + Na_2O + CaO + MgO + TiO_2)/Al_2O_3]$. Compositionally immature rocks with high ICV values tend to be found in tectonically active settings and are characteristically first-cycle deposits. Conversely, compositionally mature rocks with low ICV values are typical of tectonically quiescent or cratonic environments where sediment recycling is active, but may also be produced by intense chemical weathering of first-cycle material (Cox et al. 1995). The ICV values of the Muang Xai samples are within the range of 0.30–1.97, indicating relative compositional immaturity, consistent with being first-cycle sediments deposited in a tectonically active setting.

Successive cycles of weathering and re-deposition can increase the Th/U ratios of sedimentary rocks and are thus important indicators of weathering and sedimentary recycling (McLennan and Taylor 1980; McLennan et al. 1993). The Th/U ratios of the samples is in the 4.24–6.04 range (average of 4.83), with most samples in the 4.2–5.2 range. Such values are slightly higher than the average value of the UCC (3.8) and close to PAAS (4.97) (McLennan et al. 2006). From a diagram of Th/U-Th (Fig. 11), an increasing weathering trend can be seen, indicating a moderate degree of weathering of the source area. In the process of weathering and diagenesis, there is a significant increase in the Rb/Sr ratios of most rocks, and high values (>0.5) have been interpreted as indicators of strong weathering and recycling (McLennan et al. 1993). All of the Muang Xai samples have high Rb/Sr ratios (1.06–2.63, average of 1.79), which indicates a moderate sedimentary evolution process which is consistent with Th/U ratio results.

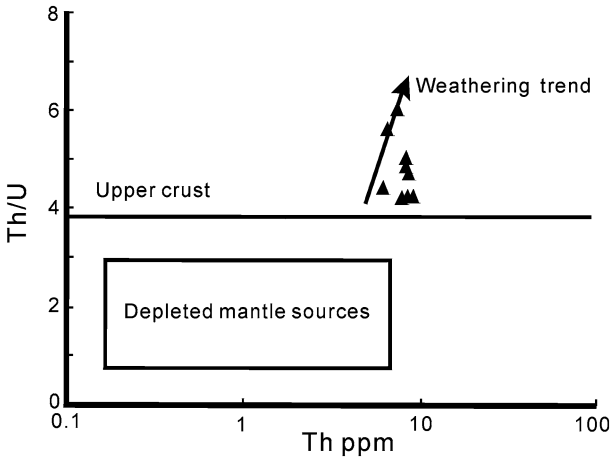


**Fig. 11** Plot of Th/U vs. Th for the sandstones from Muang Xai (after McLennan et al. 1993)

## Geochemical provenance signatures

The analysis of major elements can provide useful information about the source rocks. Roser and Korsch (1988) proposed major element discriminant functions to discriminate among four provenances where P1 = mafic source, P2 = intermediate source, P3 = felsic source and P4 = quartzose recycled source. In such a diagram (Fig. 12a), most of the samples from the Muang Xai Basin plot in the field of quartzose sediments of mature continental provenance, indicating that the sediments mainly originated from recycled continental crust. One sample plots in the intermediate field.

In the processes of weathering, erosion, and transport, insoluble trace elements are retained in the sedimentary record, and can thus provide a useful geochemical signature of the source rock (Jorge et al. 2013). Therefore, using these trace element features, it is possible to make inferences regarding the parent rocks based on the chemical compositions of the sediments, and the ratios of both compatible and incompatible elements can also be used to distinguish between felsic and mafic source components (Dostal and Keppie 2009).

Cullers (1994) concluded that Cr/Th ratios are typically in the 2.5–17.5 range for felsic rocks. All of the samples from the Muang Xai Basin have Cr/Th ratios between 1.42 and 6.05. Thus, most of the samples are likely derived from a felsic source, except for sample LM-02 (1.42). The Zr/Sc ratio is also a useful index of zircon enrichment, as zircon is strongly enriched in Zr but not Sc, which usually preserves a provenance signature (McLennan et al. 1993). Conversely, the Th/Sc ratio can distinguish the degree of igneous chemical differentiation. A diagram combining the two (Th/Sc vs. Zr/Sc) therefore provides a measure of the degree of sedimentary sorting and recycling (McLennan et al. 1993) (Fig. 12c). A portion of the Muang Xai samples evolved along the compositional variation trend in Fig. 12c, while certain samples with Hf enrichment and high Zr/Sc ratios suggest the addition of recycled zircon. In a diagram of La/Th–Hf (Fig. 12b), most samples plot in the acidic arc field and mixed felsic sources, with certain samples indicating an increasing component of old sediment.

During deposition, any variation in REE abundance patterns is significant because REE patterns are used widely for provenance characterization (McLennan 1989). Most basic rocks have lower LREE/HREE ratios and low or no Eu anomalies, whereas higher LREE/HREE ratios and negative Eu anomalies are found in felsic rocks (Cullers 1995). The Muang Xai samples exhibit Eu/Eu* ratios in the 0.58–0.71 range (average of 0.64) and LREE/HREE ratios of 6.73–12.36 (average of 9.00), indicating a mostly felsic source area, which is consistent with Eu/Eu* vs. Th/Sc (Fig. 12d).

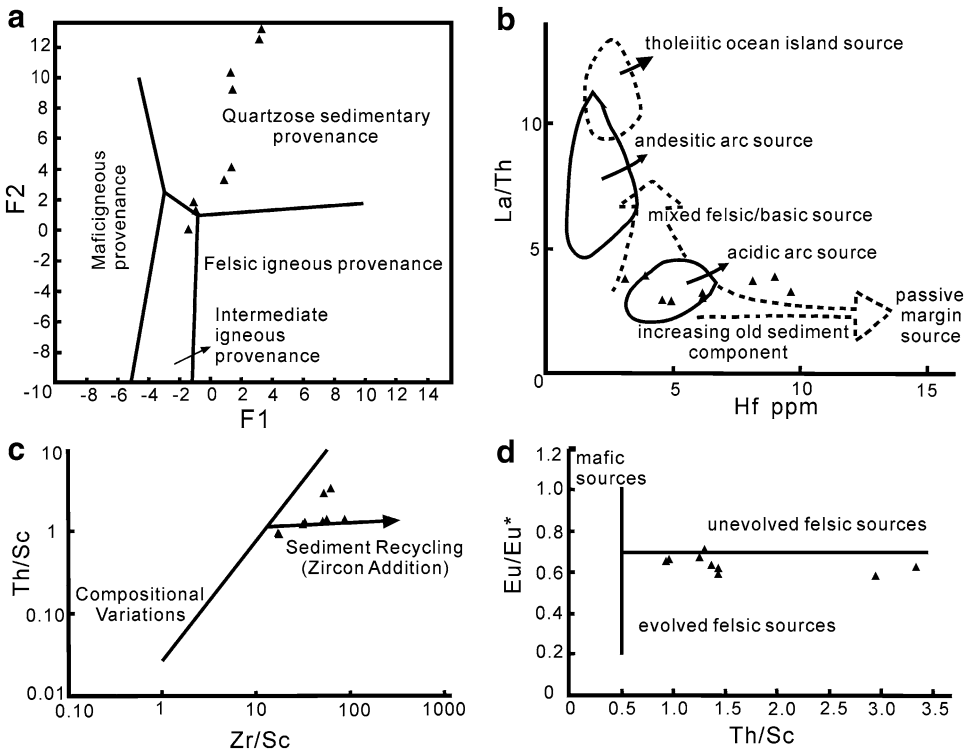


**Fig. 12** Discrimination diagrams illustrating sedimentary provenance. **a** Discrimination function diagram using major elements ratios (after Roser and Korsch 1988). **b** La/Th vs. Hf diagram using the method of Floyd and Leveridge (1987). **c** Plot of Th/Sc–Zr/Sc for the samples (after McLennan et al. 1993). **d** Eu/Eu* versus Th/Sc plot showing the samples derived from felsic sources (after McLennan et al. 1990; Jorge et al. 2013)

## Tectonic discrimination

Geochemical indicators and diagrams based on major and trace elements are used to identify the tectonic settings of sedimentary rocks (Bhatia 1983; Bhatia and Crook 1986; Roser and Korsch 1986). In Fig. 13, it is evident that the Muang Xai samples plot in three tectonic settings, but mainly in the passive continental margin field with some samples in the oceanic arc field. Two samples also plot in the continental arc field. A few samples are classified as greywacke, and thus the diagram of Th–Sc–Zr/10 (Bhatia

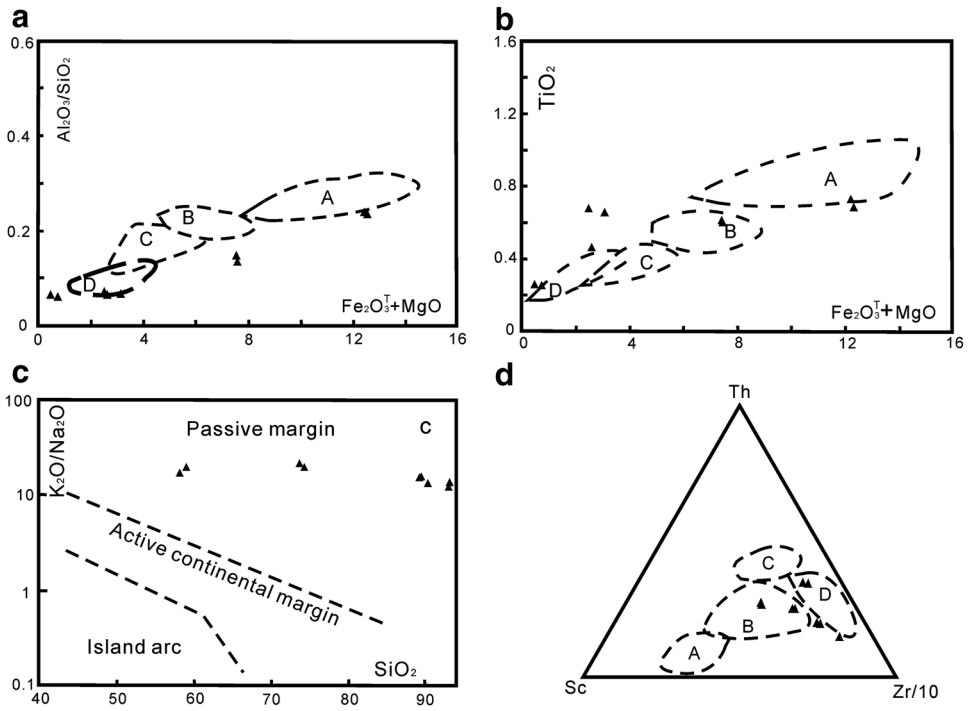


**Fig. 13** Discrimination diagrams for samples of the sandstones from the Muang Xai Basin. **a** $TiO_2$ vs. $Fe_2O_3^T + MgO$ and **b** $Al_2O_3/SiO_2$ vs. $Fe_2O_3^T + MgO$ both after Bhatia (1983); **c** $K_2O/Na_2O$ vs. $SiO^2$ after Roser and Korsch (1986); **d** Sc–Th–Zr/10 diagram after Bhatia and Crook (1986). *A* oceanic island arc, *B* continental arc, *C* active continental margin, *D* passive continental margin

and Crook 1986) is incompatible with other diagrams (Fig. 13d).

In summary, the synthesis of geochemical data indicates that the source(s) of the Muang Xai sandstones was composed mainly of felsic rocks with recycled sediment contributions. Moreover, these felsic rocks were located in an active continental margin or continental arc setting, with recycled sediment arriving from a passive continental margin.

## Detrital zircon provenance

All the zircon grains from the Muang Xai samples can be divided into four groups based on the U–Pb ages determined: Paleoproterozoic, Neoproterozoic, Ordovician–Triassic, and Jurassic–Cretaceous. Each of these groups is discussed in the following sections.

### *Provenance of Paleoproterozoic detrital zircons*

Ion microprobe (SHRIMP II) U–Pb zircon and Sm–Nd isotopic analysis provides evidence for >3.2 Ga silica crust in the Kongling Complex, northern Yangtze Craton (Qiu et al. 2000), which is coeval with the oldest zircon age (3.37 Ga) found in the Muang Xai samples. Paleoproterozoic detrital zircons (91 grains) include two sub-peaks of 1.84 Ga (1.83–1.85 Ga) and 2.48 Ga (2.47–2.50 Ga). The zircon sub-peak of 1.84 Ga exhibits high Th/U ratios (0.12–1.64) and zoning, indicating a magmatic origin (Corfu et al. 2003). Similar characteristics are observed in the zircons of 2.47–2.50 Ga which have Th/U ratios in the 0.15–1.34 range. Although a magmatic origin is inferred from the Th/U ratios, polycyclic morphology indicates that these old detrital zircons are probably recycled from Phanerozoic rocks. The Proterozoic zircons have a number of potential sources, such as the Triassic Songpan-Ganzi terrane (Weislogel et al. 2010), Neoproterozoic western Yangtze Block (Sun et al. 2009; Wang et al. 2012) and the Paleozoic south Qiangtang Block (Gehrels et al. 2011). Their ages are similar to each other (Fig. 14) and, combined with the geochemical data mentioned above, it is inferred that the recycled sediments were from a passive continental margin. Of these terranes, only the Yangtze Block was a passive margin basin in northern Gondwana (Wang and Li 2003), which is therefore consistent with the tectonic setting of the source area and it being the source of Paleoproterozoic zircons. Similarly, Carter and Bristow (2003) suggested that the source of the Cretaceous Khorat sediments was the Sichuan Basin in the Yangtze Block, while Wang et al. (2014) concluded that the Late Cretaceous sediments of the Mengyejing Formation in the Simao Basin were derived from the Yangtze Block. Therefore, the Cretaceous sediments in these basins have the same source, and the sediments of the

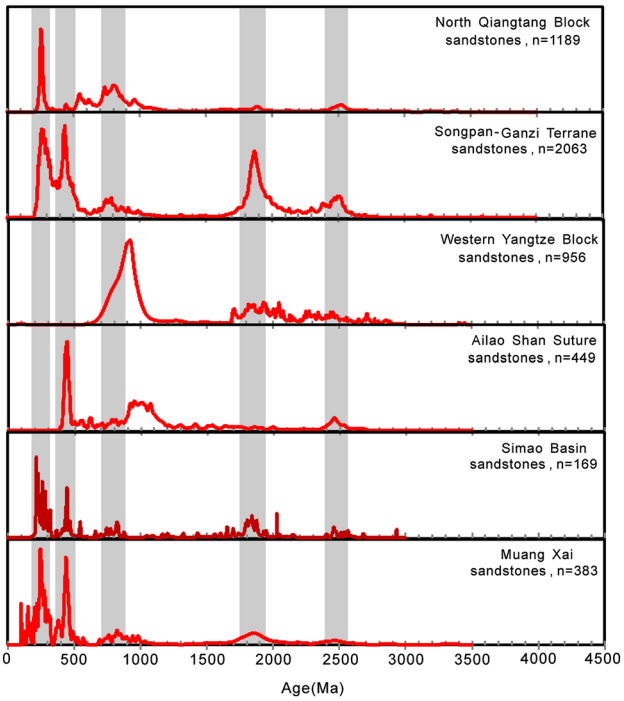


**Fig. 14** Probability density plots and histograms of LA-ICP-MS detrital zircon U–Pb ages of the Muang Xai samples compared with those from Qiangtang (Gehrels et al. 2011), Songpan-Ganzi (Weislogel et al. 2010), Yangtze (Zhao et al. 2010), Ailaoshan (Lai 2012), and Simao Basin (Wang et al. 2014)

Yangtze Block may be the source of the Paleoproterozoic polycyclic zircons. However, previous reports have indicated that similar aged detrital zircons (2.5 Ga, 1.7–2.0 Ga) also exist in the Qinling Orogenic Belt (Lease et al. 2007; Weislogel et al. 2010; Shi et al. 2013). The petrographic modal composition indicates that recycled orogenic belts are the source of the Cretaceous sandstones and, therefore, the Qinling Orogenic Belt is the likely original source of the Late Cretaceous sediments of the Muang Xai Basin.

### *Provenance of Neoproterozoic detrital zircons*

There is a Neoproterozoic zircon sub-peak age of 827 Ma, determined from 25 grains with an age range of 730–858 Ma. Previous studies indicate that Neoproterozoic magmatic rocks are widely exposed in the western Yangtze Block, such as the Shaba mafic pluton of 751 Ma (Li et al. 2003), Xuelongbao adakitic complex of 750 Ma (Zhou et al. 2006), Panzhihua gabbro of 746 and 738 Ma (Zhao and Zhou 2007), Bikou basalts of 820–810 Ma (Wang et al. 2008), and the Mopanshan adakitic complex of 780 Ma (Huang et al. 2009). Neoproterozoic magmatism related to the breakup of Rodinia (Li et al. 1995) is consistent with the detrital zircon ages of 750 to 850 Ma from Ediacaran sediments of the western Yangtze Block (Wang et al.

2012). Wang et al. (2014) also reported that the similar age of the Mengyejing Formation (740–880 Ma) in the Simao Basin may be derived from recycled Ediacaran sediments. Recycled zircons with an age range of 730–858 Ma were also possibly derived from recycled Ediacaran sediments.

*Provenance of Ordovician–Triassic detrital zircons*

A peak age of 437 Ma (416–466 Ma) was found in euhedral detrital zircons with a U/Th ratio of >0.30, which indicates a source region containing Caledonian magmatism. Some potential provenances are the Caledonian Gongbo gabbro/diabase (423–451 Ma) in the central Jinshajiang area (Jian and Liu 2002) and a xenolith in the Jinshajiang ophiolites which is 401–443 Ma in age (Jian et al. 2009). In the northeastern Muang Xai Basin, SHRIMP U–Pb ages of 400–440 Ma in the Laojunshan granitoids (Guo et al. 2009) and I-type granites in northern Laos (Wang et al. 2016) have been reported.

However, Caledonian magmatism is only present in the southeastern Yangtze Block (Wang et al. 2007, 2011; Li et al. 2010), and detrital zircons in the Devonian Guixi sandstones (Duan et al. 2012) suggest that Silurian-Early Devonian magmatism was scarce or not exhumed in the northwestern Yangtze Block (Lai 2012). Therefore, the 437 Ma detrital zircons were possibly derived from the Ailaoshan, Laojunshan, and northern Laos granitoids, and not from the basement of the Yangtze Block.

Detrital zircons in the 219–308 Ma age range ($n=92$) display a significant peaks at 248 Ma, which is Late Paleozoic to Triassic in age. Magmatism related to closure of paleo-Tethyan Ocean is extensive in the Ailaoshan suture and Truong Son Belt (Lepvier et al. 1997; Maluski et al. 2001; Peng et al. 2013) and Lincang terrane (Dong et al. 2012). Magmatic activity in the Ailaoshan suture, Truong Son Belt, and Lincang terrane may be responsible for the 219–308 Ma age clusters. The Yidun terrane can be precluded as a possible source because of the narrow Triassic age range of igneous rocks (220–240 Ma) in the eastern Yidun terrane. Recently, Yang et al. (2012b) argued that Triassic detrital zircons from the Middle Triassic turbidites in the Youjiang Basin, southeast of the Ailaoshan suture, were derived from magmatic rocks related to the Indosinian Orogeny. By this conclusion, it can be speculated that the Ailaoshan suture and Truong Son Belt were uplifted and then denuded since the Middle Triassic, thus supplying materials to form the Cretaceous sediments. This is consistent with the euhedral zoned zircons and westward directed paleocurrents in evidence (BGMRY 1986; Qu et al. 1998). It is also consistent with the geochemical results that suggest a source of felsic rocks in an active continental margin or continental arc environment.

*Provenance of Jurassic–Cretaceous detrital zircons*

There is currently no high precision isotopic age of the Mesozoic strata of the Muang Xai Basin. The youngest graphical age peak (YPP) is somewhat more compatible with depositional age than the youngest single grain age (Dickinson and Gehrels 2009). In this study, the YPP of sandstone samples is 103 Ma, which limits the stratigraphic age to no earlier than Late Cretaceous for the red beds in the Muang Xai Basin and consists of our observation in lithology associations.

Detrital zircons in the Jurassic to Cretaceous age range demonstrate two sub-peaks of 110 and 155 Ma (149–175 Ma). The 149–175 Ma detrital zircons have Th/U ratios of 0.39–0.85 and may have been derived from a proximal source, given their euhedral morphology. The 155 Ma detrital zircons were probably derived from Jurassic volcanic rocks that occur throughout Laos and Vietnam (Carter and Moss 1999) and Middle–Late Jurassic volcanic rocks of the Tule massif in northern Vietnam (176–145 Ma) (Anh et al. 2003). In Laos, equivalent sediments to the Khorat Basin overly imbricated Upper Jurassic volcanics and sedimentary rocks (Stokes et al. 1996) which point to a Late Jurassic-Early Cretaceous deformation. In central Vietnam, Lepvier et al. (1997) reported evidence for an Early Cretaceous tectonothermal event that was of sufficient intensity to cause localized deformation and epimetamorphism. Moreover, a Yanshanian magmatic-hydrothermal event (~100 Ma) and emplacement of biotite granites (110–85 Ma, Cheng and Mao 2010; Hu and Zhou 2012) occurred in the southwestern SCB (Jiang et al. 1999). Combined with the above geochemical interpretation, it is inferred that Jurassic–Cretaceous zircons were sourced from magmatic rocks of the southwestern SCB and northern Vietnam.

## Implications for the Late Cretaceous paleogeography

The Muang Xai Basin contains Cretaceous continental red beds with evaporite sequences, similar to the sedimentary facies of the Simao and Khorat Basins. Moreover, the YPP of 103 Ma suggests a Late Cretaceous age for, at least, the red beds. Therefore, it can be speculated that the continental red beds in the Muang Xai Basin are equivalent to those in the Simao Basin and, considering the geographic proximity, the Muang Xai Basin is likely a southern extension of the Simao Basin. Collectively, this is referred to as the Greater Simao Basin. The Mesozoic continental red beds are outcropped in Simao, Vientiane, and Khorat basins extending to Cambodia and to the south of Vietnam and can be correlated (Morley 2012).

However, the paleogeographic links between these basins are controversial. Carter and Bristow (2003) argued

that the Khorat Basin was located close to the Sichuan Basin in Yangtze Block at the Cretaceous time and the zircon grains were from recycled sediments of the Sichuan Basin that were originally derived from the Triassic Qinling Orogenic Belt. The view is widely accepted by most SE Asia researchers (e.g., Racey 2009; Booth and Sattayarak 2011). Paleomagnetic studies indicate differential clockwise rotation and southward displacement of the Simao and Indochina Blocks because of extrusion caused by the collision of India and Asia (Chen et al. 1995; Sato et al. 1999, 2007; Tong et al. 2013). The central Indochina Block (Khorat Basin) exhibits southward displacement of 500–1300 km (Sato et al. 1999). Recently, paleomagnetic studies from Laos and Khorat Plateau indicate a 750–1700 km latitudinal movement of the Indochina Block and suggest that the Khorat Plateau was at ca. 21–26°N and a close relation to the Sichuan Basin during the Cretaceous (Singsoupho et al. 2014). Anisotropy of magnetic susceptibility (AMS) results also suggest that the Late Cretaceous sediments in the Khorat Basin were transported mainly towards the southwest and south, into the central basin, which are sourced from the Sichuan Basin (Singsoupho et al. 2015).

The Simao Block was subjected to clockwise rotation of approximately 50° and approximately 800 km of southward displacement since the Late Eocene (Sato et al. 2007). The latest paleomagnetic data indicate that, after restoring the clockwise rotation, the Simao and Khorat are orientated approximately E–W prior to the Oligocene (Tong et al. 2013). Therefore, it is speculated that the Great Simao Basin may be located farther north than its present day approximate E–W orientation after clockwise restoration. Detrital zircon grains from the Cretaceous Khorat Group in the Khorat Basin and the Late Cretaceous Mengyejing Formation in the Simao Basin exhibit a similar distribution of U–Pb ages (Carter and Moss 1999; Floyd and Bristow 2003; Wang et al. 2014), and thus Wang et al. (2014) suggest that the Simao Basin was situated on the western margin of the Khorat Basin and pre-Devonian materials from the southwestern Sichuan Basin first supplied detritus to the Simao Basin and subsequently to the Khorat Basin during the Late Cretaceous.

The zircon age groups of the Late Cretaceous sandstones of the Muang Xai Basin are also similar to those in the Simao and Khorat basins: 2.50–2.47 Ga, 1.85–1.83 Ga, 858–730 Ma, 466–416 Ma, 308–219 Ma, 175–149 Ma, and 110–101 Ma. The 149–175 Ma subgroup from the Muang Xai Basin and the 160–170 Ma subgroup from the Khorat Basin have the same provenance, magmatic rocks in northern Vietnam. The youngest age group (101–110 Ma) may have been derived from the Late Yanshanian magmatic rocks in the southwestern Yangtze Block. This young group is distinct from the Late Cretaceous sediments of the Simao Basin.

Overall, the age patterns among the Cretaceous sediments in the three basins are similar, and their pre-Ordovician detrital zircons share the same Sichuan Basin source, as well as the Indosinian Orogeny magmatic rock origin for the Permian–Triassic zircons (Wang et al. 2014). The Jurassic–Cretaceous zircons were derived from neighboring magmatic rocks. Given that all the main detrital zircon age groups in the Simao and Khorat sediments are found in the Muang Xai sediments, in which the distinctive 110–101 Ma zircons are observed, it is suggested that the Great Simao Basin and Vientiane-Khorat Basin were not always connected. If they were, it is expected that the same detrital zircon age groups would be present in all stratigraphically equivalent sediments of these basins. Combined with the above-mentioned paleocurrent and paleomagnetic analysis, it can be indicated that sediment flowed from the Greater Simao Basin and northern Vietnam to form the Khorat red beds, and not directly from the Yangtze Block (Fig. 15) just as previously published results (Carter and Bristow 2003; Singsoupho et al. 2014, 2015).

## Conclusions

Based on the analyses of petrology, whole-rock geochemistry and detrital zircon U–Pb chronology of sandstones of the Muang Xai Basin, Laos, and the following conclusions can be drawn:

1. Petrology and geochemical data indicate that the sources of the Late Cretaceous Muang Xai sandstones were composed mainly of felsic rocks in an active continental margin or continental arc with recycled sediment derived from a passive continental margin, and that this source area was subjected to moderate weathering conditions.
2. The youngest graphical zircon age peak is 103 Ma, which gives a late Cretaceous maximum age for the Muang Xai Basin. The detrital zircon U–Pb ages reveal that pre-Ordovician zircons were derived from recycled sediments of the Yangtze Block, originally sourced from the Qinling Orogenic belt, whereas magmatic rocks of the Ailaoshan, Truong Son Belt, and Lincang terrane were responsible for zircons with peak ages of 437 and 248 Ma. Zircons with peak ages of 103 and 155 Ma were likely sourced from magmatic rocks of the southwestern SCB and northern Vietnam.
3. From provenance, paleocurrent, and paleomagnetic analyses, it can be speculated that sediment was derived from the Greater Simao Basin and northern

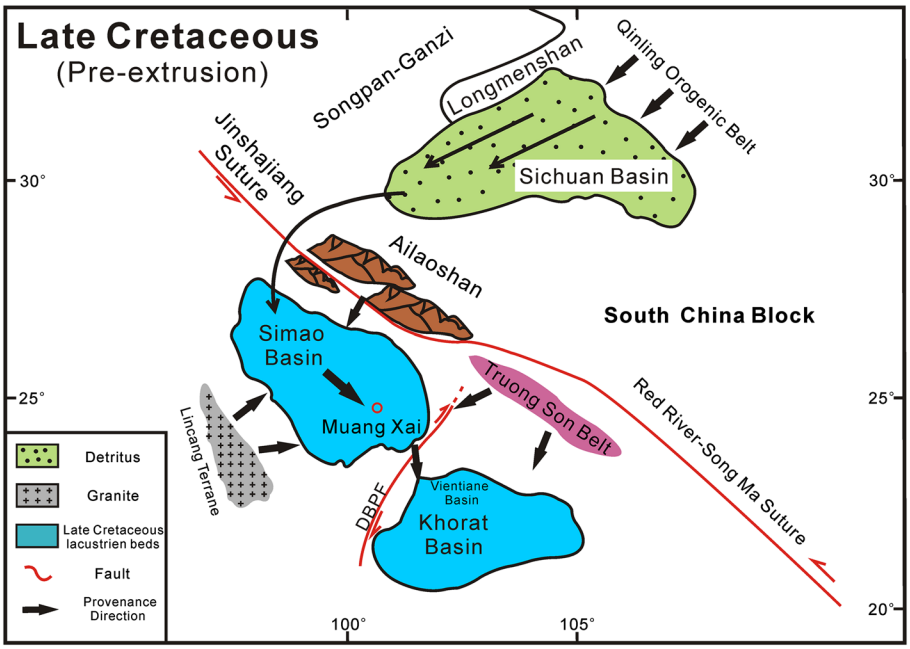


**Fig. 15** The Late Cretaceous paleogeography of the Simao and Khorat basins (Modified from Carter and Bristow 2003; Wang et al. 2014). DBPF, Dien Bien Phu Fault

Vietnam to form the Khorat red beds, and not directly from the Yangtze Block.

**Acknowledgements** This research was financially supported by the National Key Project for Basic Research of China (Project 2011CB403007) and the National Natural Science Foundation of China (No. 41572067, 41502080). We thank Professor Hu Zhaochu of China University of Geosciences in Wuhan for his assistance with the U–Pb dating and zircon trace element analyses. We are grateful to the guest editor, Prof. Hu Xiumian, and one anonymous referee for their constructive and valuable reviews which greatly improved the manuscript. Language editing by Edanz Editing Group staff is thanked for improving the English.

## References

Anh TT, Tran TH, Lan CY, Chung SL, Lo CH, Wang PL, Lee TY, Mertzman SA (2003) Geochemical and Nd–Sr isotopic constraints on the genesis of Mesozoic alkaline magmatism in the Tu Le Basin, Northern Vietnam. Geophys Res Abstr 5:02096

Belousova EA, Griffin WL, O'Reilly SY (2002) Igneous zircon: trace element composition as an indicator of source rock type. Contrib Mineral Petrol 143:602–622

Bhatia MR (1983) Plate-tectonics and geochemical composition of sandstones. J Geol 91:135–150

Bhatia MR, Crook KAW (1986) Trace elements characteristics of greywackes and tectonic setting discrimination of sedimentary basins. Contrib Mineral Petrol 92:181–193

Bock B, McLennan SM, Hanson GN (1998) Geochemistry and provenance of the middle Ordovician Austin Glen member (Normanskill formation) and the Taconian orogeny in New England. Sedimentology 45:635–655

Booth J, Sattayarak N (2011) Subsurface Carboniferous-Cretaceous geology of NE Thailand. In: Ridd MF, Barber AJ, Crow MJ (eds) The geology of Thailand. Geological Society, London, pp 185–222

Bureau of Geology and Mineral Resources of Yunnan province (BGMRY) (1986) Geology of Salt Mine in Simao area, Yunnan. Geological Publishing House, Beijing

Carter A, Bristow CS (2003) Linking hinterland evolution and continental basin sedimentation by using detrital zircon thermochronology: a study of the Khorat Plateau Basin, eastern Thailand. Basin Res 15:271–285

Carter A, Moss SJ (1999) Combined detrital-zircon fission-track and U–Pb dating: a new approach to understanding hinterland evolution. Geology 27:235–238

Chen HH, Dobson J, Heller F, Hao J (1995) Paleomagnetic evidence for clockwise rotation of the Simao region since the Cretaceous: a consequence of India-Asia collision. Earth Planet Sci Lett 134:203–217

Cheng YB, Mao JW (2010) Age and geochemistry of granites in Gejiu area, Yunnan province, SW China: constraints on their petrogenesis and tectonic setting. Lithos 120:258–276

Corfu F, Hanchar JM, Hoskin PWO, Kinny P (2003) Altas of zircon textures. Rev Mineral Geochem 53:469–500

Cox R, Lowe DR, Cullers RL (1995) The influence of sediment recycling and basement composition on evolution of mudrock chemistry in the southwestern United States. Geochemica et Cosmochimica Acta 59:2919–2940

Cullen JT, Field MP, Sherrell RM (2001) Determination of trace elements in filtered suspended marine particulate material by sector field HR-ICP-MS. J Anal At Spectrom 16:1307–1312

Cullers RL (1994) The controls on the major and trace element variation of shale, siltstone and sandstone of Pennsylvanian-Permian age from uplifted continental blocks in Colorado to platform sediment in Kansas, USA. Geochimica et Cosmochica Acta 58:4955–4972

Cullers RL (1995) The controls on the major-element and trace-element evolution of shales, siltstones and sandstones of Ordovician to Tertiary age in theWet Mountains Region, Colorado, USA. Chem Geol 12:107–131

Department of Geology and Mining, Lao P.D.R. (DGM) (1991) Geological and mineral occurrence map. 1:1000000 scale. British Geological Survey and Department of Geology and Mines

Dickinson WR, Gehrels GE (2009) Use of U–Pb ages of detrital zircons to infer maximum depositional ages of strata: a test against a Colorado Plateau Mesozoic database. Earth Planet Sci Lett 288:115–125

Dickinson WR, Suczek CA (1979) Plate tectonics and sandstone compositions. Am Assoc Pet Geol Bull 63:2164–2182

Dickinson WR, Beard LS, Brakenridge GR, Erjavec JL, Ferguson RC, Inman KF, Lindberg FA, Ryberg PT (1983) Provenance of North American Phanerozoic sandstones in relation to tectonic setting. N Am Phaneroz Sandstones 94:222–235

Dong GC, Mo XX, Zhao ZD, Zhu DC, Goodman RC, Kong HL, Wang S (2012) Zircon U–Pb dating and the petrological and geochemical constraints on Lincang granite in Western Yunnan, China: implications for the closure of the Paleo-Tethys Ocean. J Asian Earth Sci 62:282–294

Dostal J, Keppie JD (2009) Geochemistry of low-grade clastic rocks in the Acatlán Complex of southern Mexico: evidence for local provenance in felsic-intermediate igneous rocks. Sediment Geol 222:241–253

Duan L, Meng QR, Wu G, Ma SX, Li L (2012) Detrital zircon evidence for the linkage of the South China block with Gondwanaland in early Paleozoic time. Geol Mag 149:1124–1131

Fedo CM, Nesbitt HW, Young GM (1995) Unraveling the effects of potassium metasomatism in sedimentary rocks and paleosols, with implications for paleoweathering conditions and provenance. Geology 23:921–924

Fedo CM, Sircombe KN, Rainbird RG (2003) Detrital zircon analysis of the sedimentary record. Rev Mineral Geochem 53:277–303

Floyd PA, Leveridge BE (1987) Tectonic environment of the Devonian Gramscatho Basin, South Cornwall: framework mode and geochemical evidence from turbiditic sandstones. J Geol Soc London 144:531–542

Gehrels G (2012) Detrital zircon U–Pb geochronology: current methods and new opportunities. In: Busby C, Azor A (eds) Tectonics of sedimentary basins: recent advances. Wiley, Blackwell, pp 47–62

Gehrels G, Kapp P, DeCelles P, Pullen A, Blakey R, Weislogel A, Ding L, Guynn J, Martin A, McQuarrie N, Yin A (2011) Detrital zircon geochronology of pre-Tertiary strata in the Tibetan-Himalayan orogen. Tectonics 30:TC5016. doi:10.1029/2011TC002868

Guo L, Liu Y, Li C, Xu W, Ye L (2009) SHRIMP zircon U–Pb geochronology and lithogeochemistry of Caledonian Granites from the Laojunshan area, southeastern Yunnan province, China: implications for the collision between the Yangtze and Cathaysia blocks. Geochem J 43:101–122

Han YH, Ma HZ, Yuan XL, Zhang XY, Gao DL (2011) Comprehensive composition of potash deposits in Lanping-Simao Basin and Khorat Plateau. J Salt Lake Res 19:1–7 **(Chinese with English abstract)**

Haskin MA, Haskin LA (1966) Rare earths in European shales: a redetermination. Science 154:507–509

Hite RJ, Japakasetr T (1979) Potash deposits of the Khorat Plateau, Thailand and Laos. Econ Geol 74:448–458

Hoang L, Wu FY, Clift PD, Wysocka A, Swierczewska A (2009) Evaluating the evolution of the Red River system based on in situ U–Pb dating and Hf isotope analysis of zircons. Geochem Geophys Geosyst 10:Q11008. doi:10.1029/2009GC002819

Hoskin PWO, Schaltgger U (2003) The composition of zircon and igneous and metamorphic petrogenesis. Rev Mineral Geochem 53:27–55

Hu RZ, Zhou MF (2012) Multiple Mesozoic mineralization events in South China-an introduction to the thematic issue. Mineral Deposita 47:579–588

Huang XL, Xu YG, Lan JB, Yang QJ, Luo ZY (2009) Neoproterozoic adakitic rocks from Mopanshan in the western Yangtze Craton: partial melts of a thickened lower crust. Lithos 112:367–381

Ingersoll RV, Bullard TF, Ford RL, Grimm JP, Pickle JD, Sares SW (1984) The effect of grain size on detrital modes: a test of the Gazzi-Dickinson point-counting method. J Sediment Petrol 54:103–116

Jian P, Liu D (2002) U–Pb zircon dating of the Caledonian Gongbo gabbro from the Mid-Jinshajiang area, Sichuan Province. Geol Rev 48:17–21 **(in Chinese with English abstract)**

Jian P, Liu DY, Kröner A, Zhang Q, Wang YZ, Sun XM, Zhang W (2009) Devonian to Permian plate tectonic cycle of the Paleo-Tethys Orogen in southwest China (II): insights from zircon ages of ophiolites, arc/back-arc assemblages and within-plate igneous rocks and generation of the Emeishan CFB province. Lithos 113:767–784

Jiang SY, Han F, Shen JZ, Martin RP (1999) Chemical and Rb–Sr, Sm–Nd isotopic systematics of tourmaline from the Dachang Sn-polymetallic ore deposit, Guangxi Province, P.R. China. Chem Geol 157:49–67

Jorge RCGS, Fernandes P, Rodrigures B, Pereira Z, Oliveira JT (2013) Geochemistry and provenance of the Carboniferous Baixo Alentejo Flysch Group, South Portuguese Zone. Sediment Geol 284–285:133–148

Lai CK (2012) Tectonic Evolution of the Ailaoshan Fold Belt in Southwestern Yunnan, China. Ph.D Thesis University of Tasmania, Hobart, pp 1–309

Lease RO, Burbank DW, Gehrels GE, Wang ZC, Yuan DY (2007) Signatures of mountain building: detrital zircon U–Pb ages from northeastern Tibet. Geology 35:239–242

Lepvier C, Maluski H, Van Vuong N, Roques D, Axente V, Rangin C (1997) Indosinian NW-trending shear zones within the Truong Son belt (Vietnam) $^{40}Ar$–$^{39}Ar$ Triassic ages and Cretaceous to Cenozoic overprints. Tectonophysics 283:105–128

Li ZX, Zhang L, Powell CM (1995) South China in Rodinia: part of the missing link between Australia-East Antarctica and Laurentia? Geology 23:407–410

Li ZX, Li XH, Kinny PD, Wang J, Zhang S, Zhou H (2003) Geochronology of Neoproterozoic syn-rift magmatism in the Yangtze Craton, South China and correlations with other continents: evidence for a mantle super plume that broke up Rodinia. Precambrian Res 122:85–109

Li ZX, Li XH, Wartho JA, Clark C, Li WX, Zhang CL, Bao C (2010) Magmatic and metamorphic events during the early Paleozoic Wuyi-Yunkai orogeny, southeastern South China: new age constraints and pressure-temperature conditions. Geol Soc Am Bull 122:772–793

Liu YS, Hu ZC, Gao S, Günther D, Xu J, Gao CG, Chen HH (2008) In situ analysis of major and trace elements of anhydrous minerals by LA-ICP-MS without applying an internal standard. Chem Geol 257(1–2):34–43

Liu YS, Gao S, Hu ZC, Gao CG, Zong KQ, Wang DB (2010a) Continental and oceanic crust recycling-induced melt-peridotite interactions in the Trans-North China Orogen: U–Pb dating, Hf isotopes and trace elements in zircons of mantle xenoliths. J Petrol 51(1–2):537–571

Liu YS, Hu ZC, Zong KQ, Gao CG, Gao S, Xu J, Chen HH (2010b) Reappraisement and refinement of zircon U–Pb isotope and trace element analyses by LA-ICP-MS. Chin Sci Bull 55(15):1535–1546

Long X, Sun M, Yuan C, Xiao W, Cai K (2008) Early Paleozoic sedimentary record of the Chinese Altai: implications for its tectonic evolution. Sediment Geol 208:88–100

Ludwig KR (2003) ISOPLOT 3.00: a geochronological toolkit for Microsoft Excel. Berkeley Geochronology Center, California, pp 1–39

Maluski H, Lepvrier C, Jolivet L et al (2001) Ar–Ar and fission-track ages in the Song Chay Massif: early Triassic and Cenozoic tectonics in northern Vietnam. J Asian Earth Sci 19(1):233–248

McLennan SM (1989) Rare earth elements in sedimentary rocks: influence of provenance and sedimentary processes. Mineral Soc Am Rev Mineral 21:169–200

McLennan SM, Taylor SR (1980) Th and U in sedimentary rocks: crustal evolution and sedimentary recycling. Nature 285:621–624

McLennan SM, Taylor SR, McCulloch MT, Maynard JB (1990) Geochemical and Nd-Sr isotopic composition of deep-sea turbidites-crustal evolution and plate tectonic associations. Geochim Cosmochim Acta 54:2015–2050

McLennan SM, Hemming S, McDaniel DK, Hanson GN (1993) Geochemical approaches to sedimentation, provenance, and tectonics. In: Johnsson MJJ, Basu A (eds) Processes controlling the composition of clastic sediments. Geological Society of America Special Paper, New York, pp 21–40

McLennan SM, Taylor SR, Hemming SR (2006) Composition, differentiation, and evolution of continental crust: constrains from sedimentary rocks and heat flow. In: Brown M, Rushmer T (eds) Evolution and differentiation of the continental crust. Cambridge University Press, Cambridge, pp 92–134

Metcalfe I (2009) Late Palaeozoic and Mesozoic tectonic and palaeogeographical evolution of SE Asia. Geol Soc Lond 315:7–23

Metcalfe I (2011) Palaeozoic-Mesozoic history of SE Asia. In: Hall R, Cottam M, Wilson M (eds) The SE Asian gateway: history and tectonics of Australia-Asia collision. Geological Society of London Special Publications, London, pp 7–35

Metcalfe I (2013) Gondwana dispersion and Asian accretion: tectonic and palaeogeographi evolution of eastern Tethys. J Asian Earth Sci 66:1–33

Morley CK (2012) Late Cretaceous-Early Palaeogene tectonic development of SE Asia. Earth Sci Rev 115:37–75

Nesbit HW, Young YM (1984) Prediction of some weathering trends of plutonic and volcanic rocks based on thermodynamic and kinetic considerations. Geochim Cosmochim Acta 48:1523–1534

Nesbitt HW, Young GM (1982) Early Proterozoic climates and plate motions inferred from major element chemistry of lutites. Nature 299:715–717

Nesbitt HW, Young GM (1989) Formation and diagenesis of weathering profiles. J Geol 97:129–147

Nyakairu GWA, Koeberl V (2001) Mineralogical and chemical composition and distribution of rare earth elements in clay-rich sediments from central Uganda. Geochem J 35:13–28

Peng TP, Wilde SA, Wang YJ, Fan WM, Peng BX (2013) Mid-Triassic felsic igneous rocks from the southern Lancangjiang Zone, SW China: petrogenesis and implications for the evolution of Paleo-Tethys. Lithos 168–169:15–32

Pullen A, Kapp P, Gehrels GE, Vervoort JD, Ding L (2008) Triassic continental subduction in central Tibet and Mediterranean-style closure of the Paleo-Tethys Ocean. Geology 36:351–354

Qiu YM, Gao S, McNaughton NJ, Groves DI, Ling W (2000) First evidence of >3.2 Ga continental crust in the Yangtze craton of south China and its implications for Archean crustal evolution and Phanerozoic tectonics. Geology 28:11–14

Qu YH, (1997) On affinity of potassium bearing brine in Lanping-Simao Basin, China to those in Khorat Basin, Thailand. Geol Chem Mineral 19:81–84 **(in Chinese)**

Qu YH, Yuan PQ, Shuai KY, Zhang Y, Cai KQ, Jia SY, Chen CD (1998) Potash-forming rules and prospect of the Lower Tertiary in the Lanping-Simao Basin, Yunnan. Geol Publ House 1-118 **(in Chinese with English abstract)**

Racey A (2009) Mesozoic red bed sequences from SE Asia and the significance of the Khorat Group of NE Thailand. In: Buffetaut E, Cuny G, Le Loeuff J, Suteethorn V (eds) Late Palaeozoic and Mesozoic ecosystems in SE Asia. Geological Society of London Special Publications, London, pp 41–67

Racey A, Goodall JGS (2009) Palynology and stratigraphy of the Mesozoic Khorat Group red bed sequences from Thailand. In: Buffetaut E, Cuny G, Le Loeuff J, Suteethorn V (eds) Late Palaeozoic and Mesozoic ecosystems in SE Asia. Geological Society of London Special Publications, London, pp 69–83

Racey A, Love MA, Canham AC, Goodall JGS, Polachan S (1996) Stratigraphy and reservoir potential of the Mesozoic Khorat Group, North Eastern Thailand: part 1, stratigraphy and sedimentary evolution. J Pet Geol 18:5–39

Roddaz M, Viers J, Brusset S, Baby P, Boucayrand C, Herail G (2006) Controls on weathering and provenance in the Amazonian foreland basin: insights from major and trace element geochemistry of Neogene Amazonian sediments. Chem Geol 226:31–45

Roser BP, Korsch RJ (1986) Determination of tectonic setting of sandstone-mudstone suites using $SiO_2$ content and $K_2O/Na_2O$ ratio. J Geol 94:635–650

Roser BP, Korsch RJ (1988) Provenance signatures of sandstone-mudstone suites determined using discriminant function analysis of major-element data. Chem Geol 67:119–139

Sato K, Liu YY, Zhu ZC, Yang ZY, Otofuji Y (1999) Paleomagnetic study of Middle Cretaceous rocks from Yunlong, Western Yunnan, China: evidence of southward displacement of Indochina. Earth Planet Sci Lett 165:1–15

Sato K, Liu YY, Wang YB, Yokoyama M, Yoshioka S, Yang ZY, Otofuji Y (2007) Paleomagnetic study of Cretaceous rocks from Pu'er, western Yunnan, China: evidence of internal deformation of the Indochina Block. Earth Planet Sci Lett 258:1–15

Shao J, Yang S, Li C (2012) Chemical indices (CIA and WIP) as proxies for integrated chemical weathering in China: inferences from analysis of fluvial sediments. Sediment Geol 265–266:110–120

Shi Y, Yu JH, Santosh M (2013) Tectonic evolution of the Qinling orogenic belt, Central China: new evidence from geochemical, zircon U–Pb geochronology and Hf isotopes. Precambrian Res 231:19–60

Singsoupho S, Bhongsuwan T, Elming S (2014) Tectonic evaluation of the Indochina Block during Jurassic-Cretaceous from palaeomagnetic results of Mesozoic redbeds in central and southern Lao PDR. J Asian Earth Sci 92:18–35

Singsoupho S, Bhongsuwan T, Elming S (2015) Palaeocurrent direction estimated in Mesozoic redbeds of the Khorat Plateau, Lao PDR, Indochina Block using anisotropy of magnetic susceptibility. J Asian Earth Sci 106:1–18

Sone M, Metcalfe I (2008) Parallel Tethyan sutures in mainland SE Asia: new insights for Palaeo-Tethys closure. Comptes Rendus Geosci 340:166–179

Stokes RB, Lovatt-Smith PF, Soumphonphakdy K (1996) Timing of the Shan-Thai-Indochina collision: New evidence from the Pak Lay Foldbelt of the Lao PDR. In: Hall R, Blundell D (eds) Tectonic evolution of Southeast Asia, vol 106. Geological Society of London Special Publication pp 225–232

Sun WH, Zhou MF, Gao JF, Yang YH, Zhao XF, Zhao JH (2009) Detrital zircon U–Pb geochronological and Lu-Hf isotopic constraints on the Precambrian magmatic and crustal evolution of the western Yangtze Block, SW China. Precambrian Res 172:99–126

Tapponnier P, Peltzer G, Le Dain AY, Armijo R, Cobbold P (1982) Propagating extrusion tectonics in Asia: new insights from simple experiments with plasticine. Geology 10:611–616

Taylor SR, McLennan S (1985) The continental crust: its composition and evolution. Blackwell Scientific Publications, Oxford

Tong YB, Yang Z, Zheng LD, Xu YL, Wang H, Gao L, Hu XZ (2013) Internal crustal deformation in the northern part of Shan-Thai

Block: new evidence from paleomagnetic results of Cretaceous and Palaeogene red beds. Tectonophysics 608:1138–1158

Wang J, Li ZX (2003) History of Neoproterozoic rift basins in South China: implications for Rodinia break-up. Precambrian Res 122:141–158

Wang XF, Metcalfe I, Jian P, He LQ, Wang CS (2000) The Jinshajiang-Ailaoshan Suture Zone, China: tectonostratigraphy, age and evolution. J Asian Earth Sci 18:675–690

Wang Y, Fan W, Zhao G, Ji S, Peng T (2007) Zircon U–Pb geochronology of gneissic rocks in the Yunkai massif and its implications on the Caledonian event in the South China Block. Gondwana Res 12:404–416

Wang XC, Li XH, Li WX, Li ZX, Liu Y, Yang YH, Liang XR, Tu XL (2008) The Bikou basalts in the northwestern Yangtze block, South China: remnants of 820–810 Ma continental flood basalts? Geol Soc Am Bull 120:1478–1492

Wang Y, Zhang A, Fan W, Zhao G, Zhang G, Zhang Y, Li F, Li S (2011) Kwangsian crustal anatexis within the eastern South China Block: geochemical, zircon U–Pb geochronological and Hf isotopic fingerprints from the gneissoid granites of Wugong and Wuyi-Yunkai domains. Lithos 127:239–260

Wang LJ, Yu JH, Griffin WL, O'Reilly SY (2012) Early crustal evolution in the western Yangtze Block: evidence from U–Pb and Lu-Hf isotopes on detrital zircons from sedimentary rocks. Precambrian Res 222–223:368–385

Wang BQ, Wang W, Chen WT, Gao JF, Zhao XF, Yan DP, Zhou MF (2013) Constraints of detrital zircon U–Pb ages and Hf isotopes on the provenance of the Triassic Yidun Group and tectonic evolution of the Yidun Terrane, Eastern Tibet. Sediment Geol 289:74–98

Wang LC, Liu CL, Gao X, Zhang H (2014) Provenance and paleogeography of the Late Cretaceous Mengyejing Formation, Simao Basin, southeastern Tibetan Plateau: Whole-rock geochemistry, U–Pb geochronology, and Hf isotopic constraints. Sediment Geol 304:44–58

Wang LC, Liu CL, Fei MM, Shen LJ, Zhang H, Zhao YJ (2015) First SHRIMP U–Pb zircon ages of the potash-bearing Mengyejing Formation, Simao Basin, southwestern Yunnan, China. Cretaceous Res 52:238–250

Wang SF, Mo YS, Wang C, Ye PS (2016) Paleotethyan evolution of the Indochina Block as deduced from granites in northern Laos. Gondwana Res 38:183–196

Weislogel AL, Graham SA, Chang EZ, Wooden JL, Gehrels GE (2010) Detrital zircon provenance from three turbidite depocenters of the Middle-Upper Triassic Songpan-Ganzi complex, central China: record of collisional tectonics, erosional exhumation, and sediment production. Geol Soc Am Bull 122:2041–2062

Wiedenbeck M, Alle P, Corfu F, Griffin WL, Meier M, Oberli F, Quadt AV, Roddick JC, Spiegel W (1995) Three natural zircon standards for U-Th-Pb, Lu-Hf, trace element and REE analyses. Geostand Geoanal Res 19:1–23

Wu FY, Yang JH, Wilde SA, Liu XM, Guo JH, Zhai MG (2007) Detrital zircon U–Pb and Hf isotopic constraints on the crustal evolution of North Korea. Precambrian Res 159:155–177

Wu FY, Ji WQ, Liu CZ, Chung SL (2010) Detrital zircon U–Pb and Hf isotopic data from the Xigaze fore-arc basin: constraints on Transhimalayan magmatic evolution in southern Tibet. Chem Geol 271:13–25

Xu XS, Wu JL (1983) Potash deposits in Mengyejing, Yunnan:a study of certain characteristics, geochemistry of trace elements and genesis of the deposits. Acta Geoscientica Sinica 5:17–36 **(in Chinese with English abstract)**

Yang J, Cawood PA, Du Y, Huang H, Huang H, Tao P (2012a) Large igneous province and magmatic arc sourced Permian–Triassic volcanogenic sediments in China. Sediment Geol 261–262:120–131

Yang J, Cawood PA, Du Y, Huang H, Hu L (2012b) Detrital record of Indosinian mountain building in SW China: provenance of the Middle Triassic turbidites in the Youjiang Basin. Tectonophysics 574–575:105–117

Zhao JH, Zhou MF (2007) Geochemistry of Neoproterozoic mafic intrusions in the Panzhihua district (Sichuan Province, SW China): implications for subduction-related metasomatism in the upper mantle. Precambrian Res 152:27–47

Zhao XF, Zhou MF, Li JW, Sun M, Gao JF, Sun WH, Yang JS (2010) Late Paleoproterozoic to early Mesoproterozoic Dongchuan Group in Yunnan, SW China: implications for tectonic evolution of the Yangtze Block. Precambrian Res 182:57–69

Zhou MF, Yan DP, Wang CL, Qi L, Kennedy A (2006) Subduction-related origin of the 750 Ma Xuelongbao adakitic complex (Sichuan Province, China): implications for the tectonic setting of the giant Neoproterozoic magmatic event in South China. Earth Planet Sci Lett 248:286–300